Physical Communication 41 (2020) 101116

Contents lists available at ScienceDirect

Physical Communication

journal homepage: www.elsevier.com/locate/phycom

Full length article

# NOMA-based downlink relaying with media-based modulation

Mehmet Can [a,*], İbrahim Altunbaş [a], Ertugrul Basar [b]

[a] Istanbul Technical University, Faculty of Electrical and Electronics Engineering, 34469, Maslak, Istanbul, Turkey
[b] Communications Research and Innovation Laboratory (CoreLab), Department of Electrical and Electronics Engineering, Koç University, 34450, Istanbul, Turkey

ARTICLE INFO

*Article history:*
Received 3 July 2019
Received in revised form 21 March 2020
Accepted 30 April 2020
Available online 12 May 2020

*Keywords:*
Media-based modulation
Non-orthogonal multiple access
Decode-and-forward
Bit error rate

ABSTRACT

In recent years, non-orthogonal multiple access (NOMA) has attracted considerable attention as a promising multi-access technique for next generation wireless communication systems. Media-based modulation (MBM), which is an emerging index modulation concept, is another technique that can be considered for next generation wireless communication systems due to its high spectral and energy efficiency. In this paper, we propose a NOMA-based decode-and-forward relaying system, where MBM is applied at the source to improve error performance at the relay. We consider a topology consisting of a single source with a single transmit antenna equipped with multiple radio frequency (RF) mirrors, one relay equipped with a single transmit and multiple receive antennas, and multiple users equipped with multiple receive antennas. Pairwise error probability expression for NOMA with multiple receive antennas is derived and the union bound on bit error rate (BER) for the overall system with imperfect successive interference cancellation (SIC) is obtained in closed-form. Analytical results are in agreement with the Monte Carlo simulation results. Moreover, two power allocation optimization problems are formulated in terms of user fairness and quality of service requirements of the users. BER performance of the proposed system is also investigated using the optimum coefficients according to the formulated problems. It is shown that the proposed system outperforms the conventional cooperative NOMA system in terms of error performance as the data rate increases.



## 1. Introduction

Because of its high system capacity and high spectral efficiency, non-orthogonal multiple access (NOMA) is a promising multi-access technique for next-generation wireless communication networks [1]. Compared to the orthogonal multiple access (OMA) techniques, such as time division multiple access (TDMA), frequency division multiple access (FDMA) and code division multiple access (CDMA), NOMA superposes multiple users' signals to be served at the same time and frequency resources by splitting them in the power domain. In NOMA, interference is controlled by transmitting the users' signal with different allocated power levels which are based on their channel conditions. In particular, lower transmission power is allocated to users with strong channel conditions, while a higher transmission power is allocated to users with poor channel conditions. At the receiver side, users can separate their signals by using successive interference cancellation (SIC) technique where higher power allocated users' signals are decoded before their own information [2].

In recent years, NOMA has attracted remarkable attention and widely discussed in the literature. The outage probability and the ergodic sum rate performance of NOMA with randomly deployed users have been investigated in [3]. A cooperative NOMA transmission scheme is proposed and the results show that cooperative NOMA provides better performance than OMA and conventional NOMA in [4]. Due to its promising performance, many research studies have been performed on cooperative NOMA systems. Closed-form outage probability expression of NOMA amplify and forward (AF) relaying networks with multiple antennas at receivers is given in [5]. Outage performance of downlink cooperative NOMA via AF relay has been investigated for two users under Rayleigh fading channels in [6]. NOMA with AF relaying over Nakagami-*m* fading channels has been investigated in [7]. NOMA in decode and forward (DF) relaying networks is introduced in [8]. Different relay selection strategies are proposed for cooperative NOMA in [9] and [10]. Although the performance of NOMA extensively investigated in terms of outage probability, ergodic sum rate and spectral efficiency, there is a few error rate performance analysis provided in the literature. Closed-form bit error rate (BER) expression for uplink NOMA over additive white Gaussian noise (AWGN) channel is given in [11], while BER performance of uplink and downlink NOMA over fading channels is considered in [12]. The exact pairwise error probability (PEP)

* Corresponding author.
*E-mail addresses:* canmehmet@itu.edu.tr (M. Can), ibraltunbas@itu.edu.tr (İ. Altunbaş), ebasar@ku.edu.tr (E. Basar).

https://doi.org/10.1016/j.phycom.2020.101116
1874-4907/

expressions for downlink NOMA are derived and a union bound BER expression is investigated in [13].

Index modulation (IM) that provides additional information using indices of the main components of digital communication systems is another spectrum and energy efficient technique for next generation wireless communication systems [14,15]. Spatial modulation (SM) [16] and space shift keying (SSK) [17] are well-known IM applications, where indices of the available transmit antennas are used for information bits. In the literature, a number of studies combining IM and NOMA have been reported. NOMA-SM [18] and NOMA-generalized SSK schemes [19] have been proposed to mitigate inter-user interference while achieving high spectral efficiency. NOMA and SM techniques have been combined to avoid the use of the SIC method at the receiver in [20]. SM and NOMA are combined for uplink transmission in [21]. Furthermore, a novel cooperative relaying system using SM-aided NOMA is proposed in [22].

Media-based modulation (MBM) is a novel IM scheme where indices of available antenna beam patterns are used to convey information bits and it provides an attractive performance while reducing the hardware complexity [23]. While SM and SSK need significant number of transmit antennas in order to increase the data rate, MBM can achieve the same data rate even with a single transmit antenna that is equipped with multiple radio frequency (RF) mirrors or multiple electronic switches [24]. In MBM, propagation patterns of transmit antennas are changed according to the ON/OFF status of RF mirrors or electronic switches [25]. The BER performance of an SSK-MBM system is investigated over Rician fading channels in [26]. A more general concept that includes SSK and MBM techniques is introduced as channel modulation in [27]. Quadrature channel modulation concept is proposed by combining quadrature SM and MBM in [28]. The use of MBM for the uplink of a massive MIMO system is investigated in [29] and it has been shown that a BER performance can be achieved using significantly fewer antennas at the base station compared to conventional modulation. More recently, two multifunctional reconfigurable antenna designs are developed and their performances are investigated over Rayleigh fading channels in [30].

The performance of IM in relaying networks has been widely discussed in the literature. Performance analysis of SSK in DF relaying networks has been studied in [31] and [32]. The error performance of SM in relaying networks with DF protocol has been analyzed in [33] and [34]. Moreover, performance analysis of using MBM for transmission at the source and relay nodes is investigated in [35] and [36]. As seen from the previous studies in the literature, the error propagation as a result of disturbing effects in the channel between the source and the relay is an important problem for DF-based relaying networks. IM techniques can be used to reduce the impact of error propagation at the relay. Studies in [31–36] are confirmed that the use of IM schemes at the source and relay nodes provides better error performance compared to conventional modulation schemes.

Motivated by all of the above and considering hardware simplicity and remarkable error performance of MBM systems, in this paper, we propose a NOMA-based downlink relaying scheme employing the MBM technique at the source to improve the BER performance at the users by reducing error propagation at the relay.

The main contribution of this paper can be summarized as follows:

- A NOMA-based downlink relaying scheme, where MBM is employed at the source, is proposed. In this scheme, MBM is applied at the source by using a single transmit antenna and multiple RF mirrors. NOMA is applied between the DF relay and multiple users. The relay is equipped with a single transmit antenna while the relay and each mobile user are equipped with multiple receive antennas.
- The pairwise error performance of the users with multiple receive antennas is derived, and the union bound BER performance of the overall system with imperfect SIC is obtained. Moreover, the asymptotic error performance is investigated.
- Two power allocation (PA) optimization problems are formulated by using the optimization methods proposed for user fairness [37] and quality of service (QoS) requirements of the users [38].
- Our results show that the proposed system outperforms the conventional cooperative NOMA system in terms of BER performance as the data rate increases.

The rest of the paper is organized as follows. In Section 2, we describe the system model. In Section 3, the BER analysis of the NOMA-based downlink relaying with MBM at source is given. Section 4 proposes the optimal PA algorithms. The theoretical and computer simulation results are presented in Section 5. Section 6 concludes the paper.

*Notation* Bold capital and bold lowercase letters denote matrices and vectors, respectively. $(\cdot)^*$, $|\cdot|$, $\|\cdot\|$ and $\Re\{\cdot\}$ denote the complex conjugate, the absolute value, the Frobenius norm operation and the real part operator, respectively. $Pr(\cdot)$ and $f_X(\cdot)$ stand for the probability of an event and probability density function (PDF) of the random variable $X$. Moreover, $\mathcal{CN}(\mu, \sigma^2)$ denotes complex normal distribution with mean $\mu$ and variance $\sigma^2$.

## 2. System model

We consider a downlink relaying scenario, as shown in Fig. 1, where one base station (S) transmits information to $K$ mobile users, denoted by $U_1, U_2, \ldots, U_K$, with the help of a DF relay (R). At S, the MBM technique is applied by using a single transmit antenna and $M_{rf}$ RF mirrors to improve the BER performance at R. R and each mobile user are equipped with $N_R$ and $N_D$ receive antennas, respectively, while R is equipped with a single transmit antenna. The overall transmission consists of two time slots. We assume that direct links between S and mobile users are not available. Also, perfect channel state information (CSI) is available at the receiving nodes.

In the first time slot, the MBM technique is applied at S, where an MBM signal is transmitted from S to the R. The bit sequence $\mathbf{b} = [\mathbf{b}_1\ \mathbf{b}_2 \cdots\ \mathbf{b}_K]$, where $\mathbf{b}_i$ is the sequence of information bits for $U_i$, split into two parts as $\mathbf{b}^1$ and $\mathbf{b}^2$. $\mathbf{b}^1 = [\mathbf{b}_1\ \mathbf{b}_2 \cdots\ \mathbf{b}_m]$ consists of the bits of the first $m$ users and contains $M_{rf}$ bits and $\mathbf{b}^2 = [\mathbf{b}_{m+1}\ \mathbf{b}_{m+2} \cdots\ \mathbf{b}_K]$ consists of the bits of the remaining users and contains $\log_2 M$ bits. In transmission, $\mathbf{b}^1$ is used for selection of the active channel state, while $\mathbf{b}^2$ is mapped into the symbol chosen from $M$-QAM constellation diagram.

The received signal at R is expressed as

$$\mathbf{y}_R = \sqrt{P_S}\mathbf{h}_l x_q + \mathbf{n}_R \tag{1}$$

where $P_S$ is the transmit power at S, $\mathbf{h}_l$ is the $l$th column of the corresponding equivalent MBM channel matrix, $\mathbf{H} = [\mathbf{h}_1^{SR}\ \mathbf{h}_2^{SR} \cdots\ \mathbf{h}_{2^{M_{rf}}}^{SR}]$, with each element of $\mathbf{h}_m^{SR}$, $m = 1, 2, \ldots, 2^{M_{rf}}$, being independent and identically distributed (i.i.d.) as $\mathcal{CN}(0, 1)$, $x_q$ is the corresponding $M$-QAM symbol and $\mathbf{n}_R$ is the additive noise vector at R whose elements are i.i.d. random variables with $\mathcal{CN}(0, N_0)$.

The detector at R jointly estimates the active channel state index $\hat{l}$, and the $M$-QAM symbol $\hat{x}_q$, with maximum-likelihood

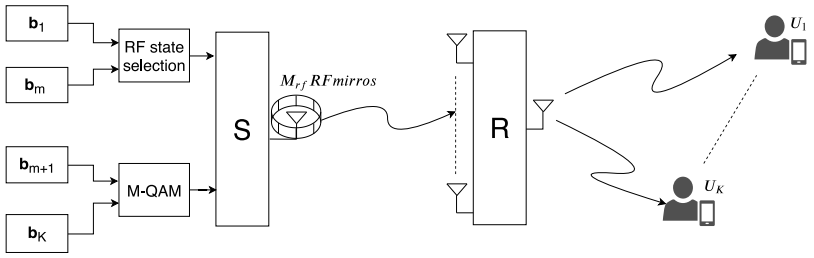


**Fig. 1.** System model with $K$ users.

(ML) decision rule, as

$$[\hat{l},\ \hat{x}_q] = \arg\min_{l,\ q} \|\mathbf{y}_R - \mathbf{h}_l\sqrt{P_S}x_q\|^2 \tag{2}$$

and decodes the bit sequence $\hat{\mathbf{b}} = [\hat{\mathbf{b}}_1\ \hat{\mathbf{b}}_2 \cdots\ \hat{\mathbf{b}}_K]$.

In the second time slot, NOMA is applied at R. Here, R uses multilevel ($L$) QAM as well and transmits the superposition symbol

$$s = \sum_{i=1}^{K} \sqrt{\alpha_i P_R}\ \hat{x}_i \tag{3}$$

to the $K$ mobile users, where $P_R$ is the transmit power at R, $\hat{x}_i$ is the corresponding $L$-QAM symbol of the $U_i$'s decoded bits $\hat{\mathbf{b}}_i$, and $\alpha_i$ is the PA coefficient of $U_i$ with $\sum_{i=1}^{K}\alpha_i = 1$. Without loss of generality, we assume that users' channel gains are ordered as $\|\mathbf{h}_{RD_1}\|^2 < \|\mathbf{h}_{RD_2}\|^2 < \cdots < \|\mathbf{h}_{RD_K}\|^2$, where $\mathbf{h}_{RD_i} = [h^1_{RD_i}\ h^2_{RD_i} \cdots\ h^{N_D}_{RD_i}]$ is the channel vector between R and $U_i$ and each element is being i.i.d. random variable as $\mathcal{CN}(0,1)$ for $i = 1, 2, \ldots, K$. Following the principle of NOMA, PA coefficients of the users are ordered as $\alpha_1 > \alpha_2 > \cdots > \alpha_K$.

The received signal at $U_i$ is

$$\mathbf{y}_i = \mathbf{h}_{RD_i}s + \mathbf{n}_i \tag{4}$$

where $\mathbf{n}_i$ is the additive noise vector at $U_i$ whose elements are i.i.d. random variables with $\mathcal{CN}(0, N_0)$.

For each user, the received signal is subject to interference by signals of other $K-1$ users. Therefore, SIC should be employed to reduce interference by eliminating higher power allocated users' signals. For example, at $U_i$, signals of $U_1, \ldots, U_{i-1}$ will be detected and subtracted from $\mathbf{y}_i$ in a successive manner and the rest of the signals of $U_{i+1}, \ldots, U_K$ will be treated as noise.

For the highest power allocated user $U_1$, signals of the other users will be treated as noise and SIC is not required. As a result, $U_1$ decodes its own signal considering ML detection as

$$\check{x}_1 = \arg\min_{x_i} \|\mathbf{y}_1 - \mathbf{h}_{RD_1}\sqrt{\alpha_1 P_R}x_i\|^2 \tag{5}$$

where $x_i$ is the possible transmitted signal from the QAM set and $\check{x}_1$ denotes decoded signal at $U_1$.

However, for $U_i$, $i > 1$, the ML detection rule becomes

$$\check{x}_i = \arg\min_{x_i} \|\mathbf{y}'_i - \mathbf{h}_{RD_i}\sqrt{\alpha_i P_R}x_i\|^2 \tag{6}$$

where $\mathbf{y}'_i$ is the output of the $i-1$ SIC iterations and given as [13]:

$$\mathbf{y}'_i = \left(\sqrt{\alpha_i P_R}\hat{x}_i + \sum_{j=1}^{i-1}\sqrt{\alpha_j P_R}\hat{\Delta}_j + \sum_{k=i+1}^{K}\sqrt{\alpha_k P_R}\hat{x}_k\right)\mathbf{h}_{RD_i} + \mathbf{n}_i \tag{7}$$

where $\hat{\Delta}_j = \hat{x}_j - \check{x}_j$ and $\check{x}_j$ denotes the decoded symbol of $U_j$.

## 3. Performance analysis

In this section, we analyze the BER performance of the proposed system by using the union bound method and PEP. Recalling that the PEP at $U_i$ depends on other users' transmitted symbols and SIC operation, to calculate the BER for $U_i$, all possible scenarios on other users' signals should be considered.

The average BER of the proposed system can be evaluated by using the union bound method [39] as follows

$$\begin{aligned} P_{e,i} \le \frac{1}{L^K}\sum_{x_{lq}}\sum_{x_{\hat{l}\hat{q}}} Pr(x_{lq} \to x_{\hat{l}\hat{q}}) \sum_{\check{x}_i} Pr\left(\hat{x}_i \to \check{x}_i | \hat{\mathbf{x}}^{(i)},\ \hat{\boldsymbol{\Delta}}^{(i)}\right) \\ \times \prod_{u=1}^{i-1} Pr\left(\hat{x}_u \to \check{x}_u | \hat{\mathbf{x}}^{(u)},\ \hat{\boldsymbol{\Delta}}^{(u)}\right) \frac{e(\mathbf{b}_i \to \check{\mathbf{b}}_i)}{\log_2(L)} \end{aligned} \tag{8}$$

where $P_{e,i}$ denotes the average BER for $U_i$, $Pr(x_{lq} \to x_{\hat{l}\hat{q}})$ is the PEP at R and stands for erroneously deciding the symbol as $\hat{x}_q$ and active channel state index as $\hat{l}$ given that the symbol $x_q$ transmitted from the active channel state $l$. Here, $2^{M_{rf}} \times M$ possible combinations of active channel states and signal constellation symbols can be obtained for $x_{lq}$. $Pr(\hat{x}_i \to \check{x}_i | \hat{\mathbf{x}}^{(i)},\ \hat{\boldsymbol{\Delta}}^{(i)})$ denotes conditional PEP at $U_i$ where $\hat{\mathbf{x}}^{(i)} = \left[\hat{x}_{i+1}, \hat{x}_{i+2}, \ldots, \hat{x}_K\right]$ and $\hat{\boldsymbol{\Delta}}^{(i)} = \left[\hat{\Delta}_1, \hat{\Delta}_2, \ldots, \hat{\Delta}_{i-1}\right]$. $e(\mathbf{b}_i \to \check{\mathbf{b}}_i)$ is the number of bits in error between transmitted and received information. Note that the product term comes from the SIC operation and the SIC error since the imperfect SIC operation degrades the BER performance.

### 3.1. Pairwise error probability at the relay

$Pr(x_{lq} \to x_{\hat{l}\hat{q}})$ is the probability of the error event at R, which corresponds to deciding $\hat{l}$ instead of $l$ for active RF mirror pattern and deciding $\hat{x}_q$ instead of $x_q$ for data symbol. Therefore, using (2) conditional PEP can be calculated as

$$Pr(x_{lq} \to x_{\hat{l}\hat{q}} \mid \mathbf{H}) = Q\left(\sqrt{\frac{P_S\|\mathbf{h}_l x_q - \mathbf{h}_{\hat{l}}\hat{x}_q\|^2}{2N_0}}\right) = Q\left(\sqrt{\kappa}\right) \tag{9}$$

where $Q(\cdot)$ is the Gaussian-Q function [39]. For flat Rayleigh fading channel, $\kappa$ follows $Gamma(N_R, \bar{\kappa})$ distribution and the PDF of $\kappa$ is given as [32]

$$f_\kappa(y) = \frac{y^{N_R-1}e^{-y/\bar{\kappa}}}{\bar{\kappa}^{N_R}(N_R-1)!} \tag{10}$$

where

$$\bar{\kappa} = \begin{cases} \frac{P_S}{2N_0}|x_q - \hat{x}_q|^2 & \text{if} \quad l = \hat{l} \\ \frac{P_S}{2N_0}\left(|x_q|^2 - |\hat{x}_q|^2\right) & \text{if} \quad l \neq \hat{l}. \end{cases} \tag{11}$$

Using the moment generating function (MGF) approach [40], unconditional PEP given in (9) can be obtained as

$$Pr(x_{lq} \to x_{\hat{i}\hat{q}}) = \frac{1}{\pi}\int_0^{\frac{\pi}{2}} M_\kappa\left(\frac{1}{2\sin^2(\theta)}\right)d\theta \tag{12}$$

where $M_\kappa(\cdot)$ is the MGF of the $\kappa$ which is expressed as [40]

$$M_\kappa(s) = \frac{1}{(1+s\bar{\kappa})^{N_R}}. \tag{13}$$

Substituting (13) into (12) and using [40, Eq.5A.4b], PEP at the relay can be computed as

$$Pr(x_{lq} \to x_{\hat{i}\hat{q}}) = \mu^{N_R}\sum_{k=0}^{N_R-1}\binom{N_R-1+k}{k}[1-\mu]^k \tag{14}$$

where $\mu = \frac{1}{2}\left(1-\sqrt{\frac{\bar{\kappa}/2}{1+\bar{\kappa}/2}}\right)$ and $\binom{\cdot}{\cdot}$ denotes the binomial coefficient.

### 3.2. Pairwise error probability at the users

$Pr\left(\hat{x}_i \to \check{x}_i|\hat{\mathbf{x}}^{(i)},\ \hat{\boldsymbol{\Delta}}^{(i)}\right)$ is the conditional probability of the error event at $U_i$, which corresponds to deciding symbol $\check{x}_i$ instead of the transmitted symbol $\hat{x}_i$ from R and conditioned on other users' symbols and SIC detection. Conditional PEP for $U_i$ is given by [13]

$$Pr\left(\hat{x}_i \to \check{x}_i|\hat{\mathbf{x}}^{(i)},\ \hat{\boldsymbol{\Delta}}^{(i)}, \mathbf{h}_{RD_i}\right) = Q\left(\frac{\|\mathbf{h}_{RD_i}\|\beta_i}{\nu_i}\right) \tag{15}$$

where $\beta_i$ and $\nu_i$ are given as

$$\beta_i = \sqrt{\alpha_i P_R}|\hat{\Delta}_i|^2 + 2\Re\left\{\hat{\Delta}_i\left[\sum_{u=1}^{i-1}\sqrt{\alpha_u P_R}\hat{\Delta}_u^* + \sum_{\hat{j}=i+1}^{K}\sqrt{\alpha_j P_R}\hat{x}_j^*\right]\right\} \tag{16}$$

and

$$\nu_i = \sqrt{2}N_0|\hat{\Delta}_i|. \tag{17}$$

$Pr\left(\hat{x}_i \to \check{x}_i|\hat{\mathbf{x}}^{(i)},\ \hat{\boldsymbol{\Delta}}^{(i)}\right)$ can be calculated by replacing $\kappa$ by $\kappa_i = \frac{\|\mathbf{h}_{RD_i}\|^2\beta_i^2}{\nu_i^2}$ in (12). Therefore, we should first derive the $M_{\kappa_i}(s)$ expression.

For flat Rayleigh fading channel unordered $\kappa_i$ follows *Gamma* $(N_D, \bar{\kappa}_i)$ distribution where $\bar{\kappa}_i = \frac{\beta_i^2}{\nu_i^2}$. The PDF and the cumulative distribution function (CDF) of the unordered $\kappa_i$ are given by

$$f_{\bar{\kappa}_i}(y) = \frac{y^{N_D-1}e^{-y/\bar{\kappa}_i}}{\bar{\kappa}_i^{N_D}(N_D-1)!} \tag{18}$$

$$F_{\bar{\kappa}_i}(y) = 1 - e^{-y/\bar{\kappa}_i}\sum_{m=0}^{N_D-1}\frac{1}{m!}(y/\bar{\kappa}_i)^m. \tag{19}$$

Therefore, the PDF of the ordered variable $\kappa_i$ can be calculated as

$$\begin{aligned} f_{\kappa_i}(y) &= \frac{K!}{(K-i)!(i-1)!}f_{\bar{\kappa}_i}(y)\left[F_{\bar{\kappa}_i}(y)\right]^{i-1}\left[1-F_{\bar{\kappa}_i}(y)\right]^{K-i} \\ &= \frac{K!}{(K-i)!(i-1)!}\sum_{k=0}^{i-1}(-1)^k\binom{i-1}{k}\frac{e^{-y/\bar{\kappa}_i}(y/\bar{\kappa}_i)^{N_D-1}}{\bar{\kappa}_i(N_D-1)!} \\ &\times e^{-y(K-i+k)/\bar{\kappa}_i}\left[\sum_{m=0}^{N_D-1}\frac{1}{m!}(y/\bar{\kappa}_i)^m\right]^{K-i+k}. \end{aligned} \tag{20}$$

Applying successive binomial expansions and denoting $b_m = \frac{1}{m!\bar{\kappa}_i^m}$ and $\alpha = K-i+k$, last term in (20) can be written as [5]:

$$\begin{aligned} \Phi &= \left[\sum_{m=0}^{N_D-1}b_m y^m\right]^\alpha = \left[b_0 + \sum_{m=1}^{N_D-1}b_m y^m\right]^\alpha = \sum_{k_1=0}^{\alpha}\binom{\alpha}{k_1}b_0^{k_1}\left[\sum_{m=1}^{N_D-1}b_m y^m\right]^{\alpha-k_1} \\ &= \sum_{k_1=0}^{\alpha}\binom{\alpha}{k_1}b_0^{k_1}\sum_{k_2=0}^{\alpha-k_1}\binom{\alpha-k_1}{k_2}(b_1y)^{k_2}\left[\sum_{m=2}^{N_D-1}b_m y^m\right]^{\alpha-k_1-k_2} \\ &= \sum_{k_1=0}^{\alpha}\sum_{k_2=0}^{\alpha-k_1}\cdots\sum_{k_{N_D-1}=0}^{\alpha-k_1-\cdots-k_{N_D-2}}\binom{\alpha}{k_1}\binom{\alpha-k_1}{k_2}\cdots\binom{\alpha-k_1-\cdots-k_{N_D-2}}{k_1} \\ &\times b_0^{k_1}(b_1y)^{k_2}(b_2y)^{k_3}\cdots(b_{N_D-2}y^{N_D-2})^{k_{N_D-1}}(b_{N_D-1}y^{N_D-1})^{\alpha-k_1-\cdots-k_{N_D-1}}. \end{aligned} \tag{21}$$

Substituting (21) into (20), $M_{\kappa_i}(s)$ can be given as

$$\begin{aligned} M_{\kappa_i}(s) &= \int_0^\infty e^{-sy}f_{\kappa_i}(y)dy \\ &= \frac{K}{\bar{\kappa}_i^{N_D}(N_D-1)!}\sum_{k=0}^{i-1}\bigcup_{k'}(-1)^k U_{k'}V_{k'}\int_0^\infty e^{-\left(s+\frac{\alpha+1}{\bar{\kappa}_i}\right)y}y^{N_D+\bar{k}-1}dy \end{aligned} \tag{22}$$

where $\bigcup_{k'} \triangleq \sum_{k_1=0}^{\alpha}\sum_{k_2=0}^{\alpha-k_1}\cdots\sum_{k_{N_D-1}=0}^{\alpha-k_1-\cdots-k_{N_D-2}}$, $U_{k'} = \binom{K-1}{i-1}\binom{i-1}{k}\times\binom{\alpha}{k_1}\binom{\alpha-k_1}{k_2}\cdots\binom{\alpha-k_1-\cdots-k_{N_D-2}}{k_1}$, $V_{k'} = b_{N_D-1}^{\alpha-k_1-\cdots-k_{N_D-1}}\prod_{m=0}^{N_D-2}b_m^{k_{m+1}}$, and $\bar{k} = (N_D-1)(\alpha-k_1)-(N_D-2)k_2-(N_D-3)k_3-\cdots-k_{N_D-1}$.

Using [41, Eq.3.381.4], $M_{\kappa_i}(s)$ can be rewritten in closed-form as

$$M_{\kappa_i}(s) = \frac{K}{\bar{\kappa}_i^{N_D}(N_D-1)!}\sum_{k=0}^{i-1}\bigcup_{k'}(-1)^k U_{k'}V_{k'}\frac{\Gamma(N_D+\bar{k})}{\left(\frac{s+(\alpha+1)}{\bar{\kappa}_i}\right)^{N_D+\bar{k}}} \tag{23}$$

where $\Gamma(\cdot)$ denotes the complete gamma function.

Substituting (23) into (12) and using [41, Eq.3.682, Eq.8.384], the conditional PEP at $U_i$ can be computed as

$$\begin{aligned} Pr(\hat{x}_i \to \check{x}_i|\hat{\mathbf{x}}^{(i)},\ \hat{\boldsymbol{\Delta}}^{(i)}) &= \frac{K}{\bar{\kappa}_i^{N_D}(N_D-1)!}\sum_{k=0}^{i-1}\bigcup_{k'}(-1)^k U_{k'}V_{k'}Q_k \\ &\times\frac{\Gamma(2(N_D+\bar{k}))}{\Gamma(N_D+\bar{k}+1)}{}_2F_1\left(\frac{1}{2}, N_D+\bar{k}; N_D+\bar{k}+1; \frac{2\alpha+2}{\bar{\kappa}_i+2\alpha+2}\right) \end{aligned} \tag{24}$$

where $Q_k = \frac{2}{\left(4+\frac{(\alpha+1)}{\bar{\kappa}_i}\right)^{N_D+\bar{k}}}$ and ${}_2F_1(\cdot,\cdot;\cdot;\cdot)$ denotes Gauss hypergeometric function [41].

By substituting (14) and (24) into (8), the average BER of the proposed scheme can be obtained. Since the final expression is relatively long and complicated, we omitted this for the clarity of the presentation.

### 3.3. Asymptotic error probability analysis

In this subsection, we analyze the asymptotic BER performance of the proposed system. In this regard, we investigate the previously derived PEP results at high SNR values to calculate the asymptotic PEP at the relay and users, respectively.

#### 3.3.1. Asymptotic pairwise error probability at the relay

The MGF of $\kappa$ can be approximated at high SNR values as

$$M_\kappa(s) \approx \left(\frac{1}{s\bar{\kappa}}\right)^{N_R}. \tag{25}$$

Substituting (25) into (12) and using [41, Eq.3.621, Eq.8.384] asymptotic PEP at the relay can be computed as

$$Pr(x_{lq} \to x_{\hat{l}\hat{q}}) \approx \frac{2^{N_R-1}\Gamma(N_R+\frac{1}{2})}{\sqrt{\pi}\bar{\kappa}^{N_R}\Gamma(N_R+1)}. \tag{26}$$

At the high SNR values, the PEP expression can be approximately written as [42]

$$Pr(x_{lq} \to x_{\hat{l}\hat{q}}) \approx (G_c\bar{\kappa})^{-G_d} \tag{27}$$

where $G_c$ and $G_d$ are coding and diversity gain, respectively.

From (26), the diversity gain of the transmission from S to R can be obtained as $G_d = N_R$, and the coding gain can be derived as

$$G_c = \left(\frac{2^{N_R-1}\Gamma(N_R+\frac{1}{2})}{\sqrt{\pi}\Gamma(N_R+1)}\right)^{-\frac{1}{N_R}}. \tag{28}$$

As clearly seen, $N_R$ is an important factor for both diversity and coding gains at the relay. Increasing $N_R$ increases these gains as well.

*3.3.2. Asymptotic pairwise error probability at the users*

For high SNR values, the PDF and CDF of unordered $\kappa_i$ are asymptotically given by

$$f_{\bar{\kappa}_i}(y) \approx \frac{y^{N_D-1}}{\bar{\kappa}^{N_D}(N_D-1)!} \tag{29}$$

$$F_{\bar{\kappa}_i}(y) \approx \frac{y^{N_D}}{\bar{\kappa}^{N_D}N_D!}. \tag{30}$$

Substituting (29) and (30) into (20), the PDF of the ordered $\kappa_i$ can be approximated as

$$f_{\kappa_i}(y) \approx \frac{K!}{(K-i)!(i-1)!}\frac{N_D y^{iN_D-1}}{\bar{\kappa}_i^{iN_D}(N_D!)^i}. \tag{31}$$

Using (31), the MGF can be approximated as

$$M_{\kappa_i}(s) \approx \frac{K!}{(K-i)!(i-1)!}\frac{N_D\Gamma(iN_D)}{s^{iN_D}\kappa_i^{iN_D}(N_D!)^i}. \tag{32}$$

Substituting (32) into (12) and using [41, Eq.3.621, Eq.8.384], the conditional asymptotic PEP at $U_i$ can be computed as

$$Pr(\hat{x}_i \to \check{x}_i|\hat{\mathbf{x}}^{(i)},\ \hat{\boldsymbol{\Delta}}^{(i)}) \approx \frac{K!}{(K-i)!(i-1)!}\frac{2^{iN_D-1}\Gamma(iN_D+\frac{1}{2})}{\sqrt{\pi}i\bar{\kappa}^{iN_D}(N_D!)^i}. \tag{33}$$

From (33), the diversity gain of the transmission from R to $U_i$ can be obtained as $G_{d,i} = iN_D$, and the coding gain can be derived as

$$G_{c,i} = \left(\frac{K!}{(K-i)!(i-1)!}\frac{2^{iN_D-1}\Gamma(iN_D+\frac{1}{2})}{\sqrt{\pi}i(N_D!)^i}\right)^{-\frac{1}{iN_D}}. \tag{34}$$

It can be observed from these expressions that both user order and $N_D$ significantly affect the coding and diversity gains at the users. In addition to increasing $N_D$, the higher ordered user has higher coding and diversity gains.

By substituting (26) and (33) into (8), the asymptotic BER expression of the proposed system can be obtained. According to this asymptotic BER analysis, the achievable diversity gain of the system at the high SNR regime can be given as $G_{d,i} = \min\{N_R, iN_D\}$. As we will show in Figs. 3 and 4, in the following section, increasing $N_R$, $N_D$ and user order increases the diversity and/or coding gain of the overall system as well, hence provides significant SNR gains.

## 4. Power allocation optimization

In NOMA systems, PA is an important factor in achieving satisfactory performance for all users. In this section, two optimization problems are formulated by using the optimization methods proposed in the literature for user fairness and QoS requirements of the users.

PA can be designed to enhance user fairness. In [37], the authors have studied max–min fairness in NOMA to achieve the same data rate among all users. Firstly, we formulate the optimization problem for user fairness by considering the users' BERs:

$$\begin{aligned} \text{Minimize} \quad & \max\{P_{e,i}\} && ,\forall i = 1,2,\ldots,K \\ \text{s.t.} \quad & \sum_{i=1}^{K}\alpha_i = 1 \\ & \alpha_1 > \alpha_2 > \cdots > \alpha_K. \end{aligned} \tag{35}$$

When the above optimization problem is considered, the performance of the user with a strong channel condition is close to the performance of the users with poor channel conditions.

Besides user fairness, in many practical communication scenarios, users have different QoS requirements [38]. Secondly, we formulate the optimization problem for increasing the performance of the lowest power allocated user, which has a strong channel condition, while the other users satisfying specific BERs:

$$\begin{aligned} \text{Minimize} \quad & P_{e,K} \\ \text{s.t.} \quad & \sum_{i=1}^{K}\alpha_i = 1 \\ & \alpha_1 > \alpha_2 > \cdots > \alpha_K \\ & P_{e,i} < P_{th,i} && ,\forall i = 1,2,\ldots,K-1 \end{aligned} \tag{36}$$

Note that the PA coefficients can be calculated by using numerical methods such as brute-force searching since analytical solutions to optimization problems in (35) and (36) are hard to derive.

## 5. Numerical results

In this section, we present numerical and Monte Carlo simulation results for the BER performance of the proposed system. Unless otherwise stated, we set the same spectral efficiency $\eta$ for all users, the receive antennas at R and at the users are the same as $N_R = N_D = N_r$ and transmit power at S and R are equal as $P_R = P_S = P$. NOMA applied at R and the modulation order is set as $L = 2^\eta$ for $U_i$.

Fig. 2 compares the BER performance of the proposed system with the conventional cooperative NOMA system for different spectral efficiencies and for $N_r = 4$ in the case of two users. At S, $M_{rf} = 1$, 2 and 4, $M = 2$, 4 and 16 for the proposed system, and $M$-QAM modulation applied for conventional cooperative NOMA with $M = 4$, 16 and 256 for $\eta = 1$, 2 and 4 b/s/Hz, respectively. At R, PA coefficients have been arbitrarily chosen as $\alpha_1 = 0.8$, 0.85 and 0.97, $\alpha_2 = 0.2$, 0.15 and 0.03 for $\eta = 1$, 2 and 4 b/s/Hz, respectively. As seen in Fig. 2, the conventional system performs slightly better than the proposed system for $\eta = 1$ b/s/Hz. However, the proposed system provides much better performance for all users compared to the conventional system as $\eta$ values increase because MBM provides better BER performance at higher bandwidth efficiency compared to conventional modulation schemes. In particular, at a BER value of $10^{-4}$ and for $\eta = 2$ b/s/Hz, proposed system provides approximately 2.5 dB SNR gain for each user. At the $\eta = 4$ b/s/Hz, the proposed system provides approximately 5 dB and 1 dB SNR gain for $U_1$ and $U_2$, respectively. Because of its small PA coefficient and the SIC operation, the performance of $U_2$ is slightly inferior with

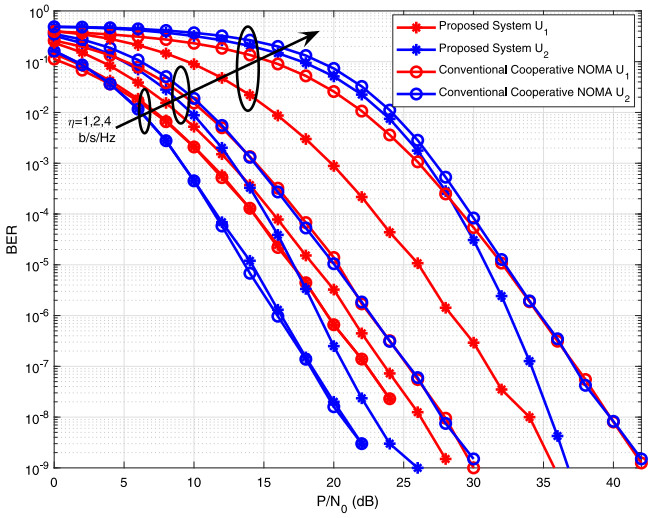


**Fig. 2.** BER performance comparison of the proposed system with the conventional cooperative NOMA system for $\eta = 1$, 2 and 4 b/s/Hz and $N_r = 4$.

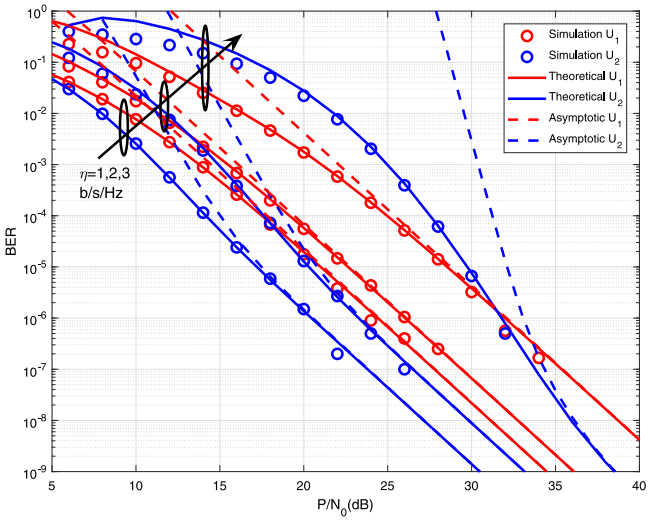


**Fig. 3.** BER performance of the proposed system for $\eta = 1$, 2, and 3 b/s/Hz, $N_r = 3$.

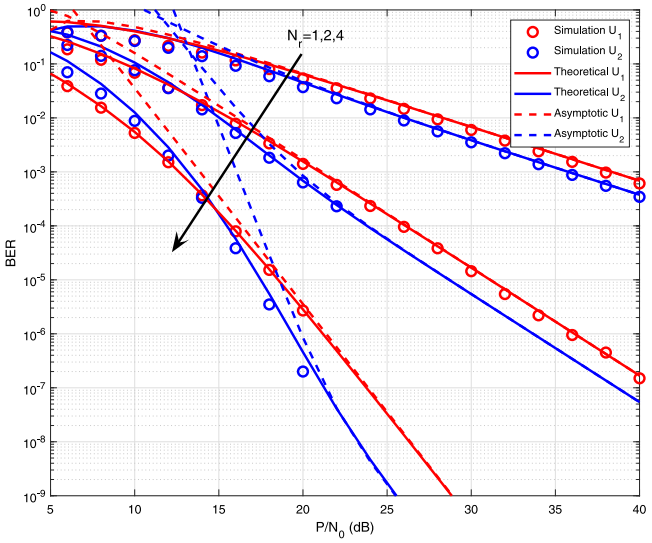


**Fig. 4.** BER performance of the proposed system for $N_r = 1$, 2, and 4, $\eta = 2$ b/s/Hz.

respect to $U_1$ at low and moderate SNR values. However, $U_2$ will provide better performance than even $U_1$ at high SNR values due to its better channel conditions. At high SNR values, the proposed system will provide a more significant gain for $U_2$ compared to the conventional system.

In Fig. 3, the BER performance of the proposed system is given for $\eta = 1$, 2 and 3 b/s/Hz where $N_r = 3$. At S, $M_{rf} = 1$, 2 and 3, $M = 2$, 4 and 8 for $\eta = 1$, 2 and 3 b/s/Hz, respectively. At R, PA coefficients have been chosen as $\alpha_1 = 0.8$, 0.85 and 0.95, $\alpha_2 = 0.2$, 0.15 and 0.05 for $\eta = 1$, 2 and 3 b/s/Hz, respectively. It is shown in Fig. 3 that the derived union bound expressions, evaluated from (8), become very tight with increasing SNR for all $\eta$ values. In addition, the asymptotic BER expressions are well-matched at the high SNR regime. Even if less power is allocated to $U_2$ than $U_1$, $U_2$ will perform better BER performance with increasing SNR since it has better channel condition. Because of the allocated power for $U_2$ decreases with increasing $\eta$ values, the BER performance of $U_2$ outperforms $U_1$ at higher SNR. For example, $U_2$ outperforms $U_1$ at 5, 13 and 32 dB for $\eta = 1$, 2 and 3, respectively. Moreover, we can observe from the high SNR regime that the diversity gains of the users are $G_{d,1} = G_{d,2} = N_r = 3$ for all $\eta$ values.

In Fig. 4, the BER performance of the proposed system is given for $N_r = 1$, 2 and 4 where $\eta = 2$ b/s/Hz, and PA coefficients are $\alpha_1 = 0.85$ and $\alpha_2 = 0.15$. As seen from Fig. 4, the analytical results are in agreement with the computer simulation results with increasing SNR and the asymptotic results are very tight at the high SNR regime. From Fig. 4, it is observed that the BER performance of all users has significantly improved by increasing receive antenna numbers. Moreover, the diversity gains of the users are $G_{d,1} = G_{d,2} = N_r$.

In Fig. 5, BER performance for three users case is investigated at $\eta = 1$ and 2 b/s/Hz where $N_r = 2$. At S, $M_{rf} = 2$ and 4, $M = 2$ and 4 for $\eta = 1$ and 2 b/s/Hz, respectively. At R, PA coefficients have been chosen as $\alpha_1 = 0.7$, $\alpha_2 = 0.24$ and $\alpha_3 = 0.06$. As seen from Fig. 5(a), the union bound provides exactly the same result with simulation results for $\eta = 1$ b/s/Hz. From Fig. 5(b), union bounds become very tight with increasing SNR for $\eta = 2$ b/s/Hz.

The optimum PA for the case of two users is investigated in Fig. 6 according to the formulated optimization problems in (35) and (36) for $\eta = 2$ b/s/Hz and $N_r = 4$. BER union bounds are evaluated for $U_1$ and $U_2$ at $\frac{P}{N_0} = 5$, 15 and 25 dB over $\alpha_2$ with step size 0.005 and are shown in Fig. 6(a). It can be seen from Fig. 6 that $U_2$ can achieve the best performance at $\alpha_2 = 0.2$ and the performance of $U_2$ decreases with increasing $\alpha_2$ after this value for each $\frac{P}{N_0}$. It is because the signal of $U_1$ is erroneously detected due to imperfect SIC and this causes error propagation. $U_1$ attains lower BER when $\alpha_2$ approaches to zero because of negligible interference from $U_2$. However, $U_2$ performs poor BER for this scenario, hereby, user fairness is not satisfied. Moreover, the optimum PA coefficients are calculated by brute-force search method according to the first ($A_1$) and second ($A_2$) optimization problem, which are based on user fairness and QoS requirements of the users, respectively, from the evaluated union bounds. From Fig. 6(a), the optimum PA coefficients are at the point where union bounds are closest to each other for $A_1$. The optimum PA coefficients for $A_1$ are $\alpha_2 = 0.155$, 0.15, 0.09 at $\frac{P}{N_0} = 5$, 10, 20 dB, respectively. For $A_2$, the threshold BER for $U_2$ is determined according to the achieved fairness BER ($P_{e,f}$) value in $A_1$ as $P_{th,1} = P_{e,f} \times 10^{0.5}$. As can be seen from Fig. 6(a), the optimum PA coefficients for $A_2$ are $\alpha_2 = 0.175$, 0.19, 0.14 at $\frac{P}{N_0} = 5$, 10, 20

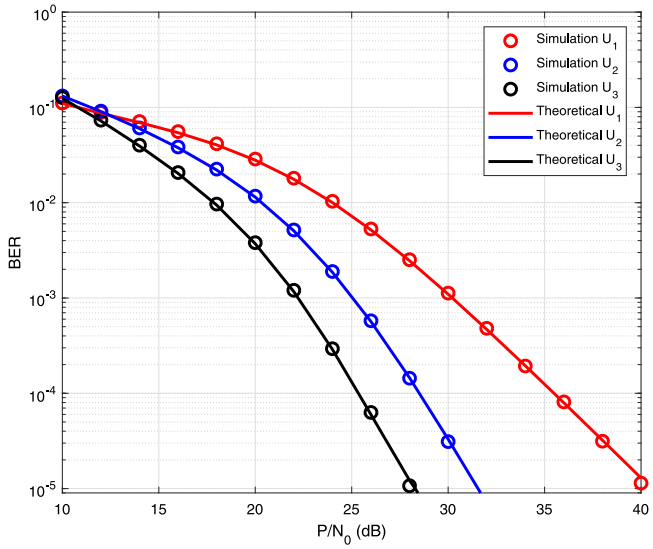


(a)

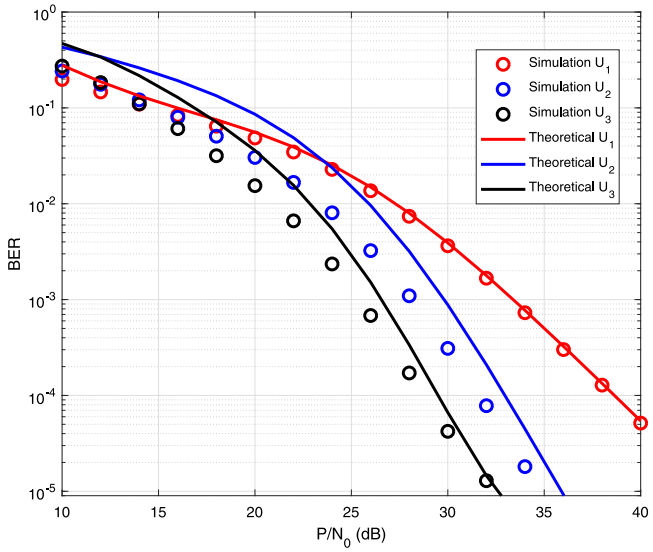


(b)

**Fig. 5.** BER performance of the proposed system for three user, $\eta = 1$ and 2 b/s/Hz, $N_r = 2$. (a) BER curves for $\eta = 1$ b/s/Hz. (b) BER curves for $\eta = 2$ b/s/Hz.

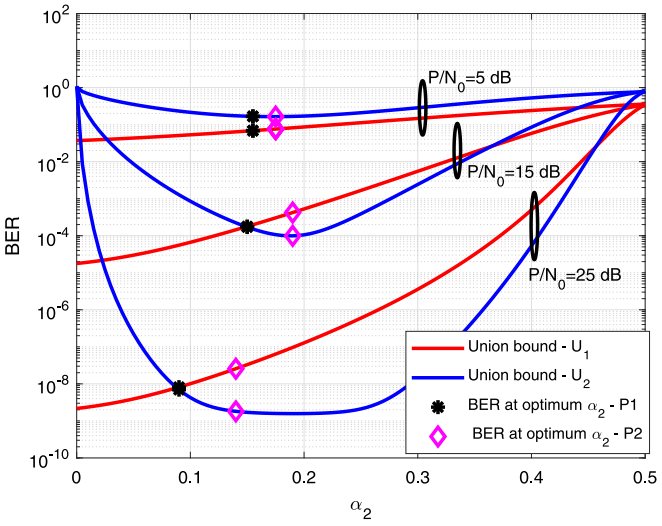


(a)

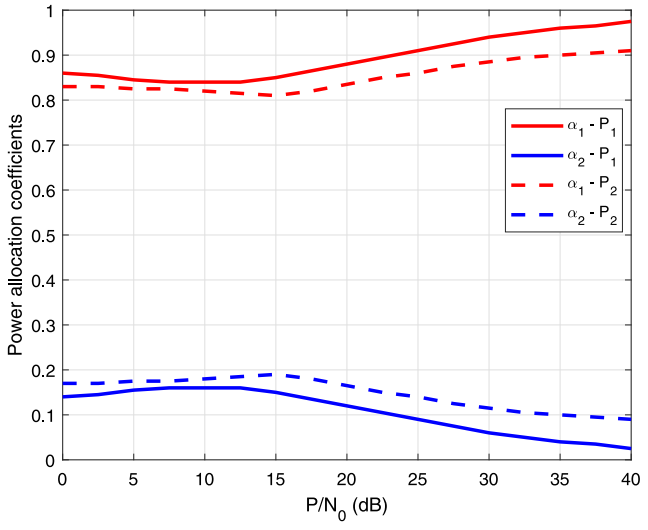


(b)

**Fig. 6.** PA optimization for two users case where $\eta = 2$ b/s/Hz and $N_r = 4$. (a) BER union bounds for $U_1$ and $U_2$ over $\alpha_2$ for $\frac{P}{N_0} = 5, 15, 20$ dB. (b) The optimal PA coefficients over $\frac{P}{N_0}$ according to PA algorithms $A_1$ and $A_2$.

dB, respectively. Moreover, the optimum PA coefficients over $\frac{P}{N_0}$ for $A_1$ and $A_2$ are shown in Fig. 6(b). From Fig. 6, as increased the $\frac{P}{N_0}$, PA coefficient for $U_1$ increases for both algorithms $A_1$ and $A_2$.

In Fig. 7, BER performance of the proposed system is investigated with the optimal PA coefficients according to $\frac{P}{N_0}$ values. As seen from Fig. 7, when PA coefficients are chosen according to $A_1$, the same BER performance for both users is provided after $\frac{P}{N_0} = 14$ dB. When coefficients are chosen according to $A_2$, BER performance of $U_2$ is increased while the threshold BER value for $U_1$ is ensured and a 1 dB SNR gain is provided.

## 6. Conclusion

In this paper, we have proposed an NOMA-based downlink relaying system with MBM at source. The PEP expression of the NOMA system with multiple receive antennas at users is derived. Moreover, the analytical BER of the overall system has been obtained by using the union bound method. It has been proved that the analytical and simulation results match very well. Then, the performance of the proposed system has been compared with conventional cooperative NOMA and it has been shown that the proposed system outperforms the conventional cooperative NOMA system in terms of BER as data rate increases. Furthermore, the effect of the PA coefficients has been investigated. Additionally, two optimization problems that aim to find the optimum PA coefficients in terms of user fairness and QoS requirements of the users are formulated. Finally, BER performances with optimum PA coefficients for both algorithms have been investigated. Our results have revealed that the use of MBM is a promising technique for NOMA-based relaying systems with its remarkable error performance and hardware simplicity. Our

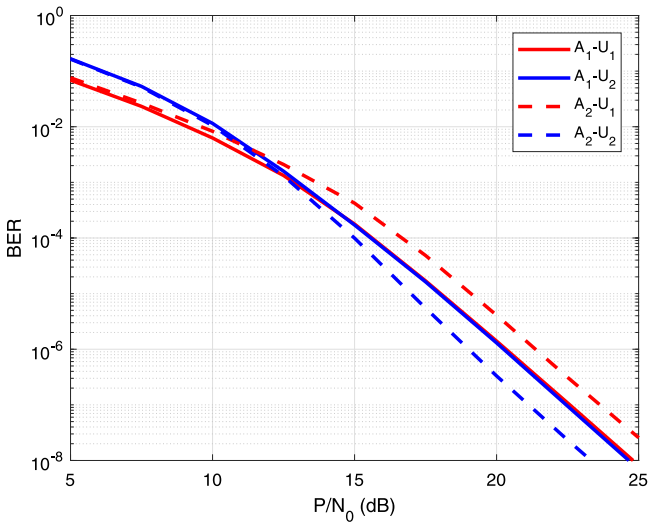


**Fig. 7.** BER performance with the optimal PA coefficients for each $\frac{P}{N_0}$ value according to PA algorithms $A_1$ and $A_2$.

future work will focus on designing new transmission schemes that allow the use of MBM in both the source and the relay in cooperative NOMA systems.

## CRediT authorship contribution statement

**Mehmet Can:** Conceptualization, Methodology, Software, Validation, Investigation, Writing - original draft, Writing - review & editing. **İbrahim Altunbaş:** Conceptualization, Methodology, Writing - review & editing, Project administration, Supervision. **Ertugrul Basar:** Conceptualization, Methodology, Writing - review & editing, Project administration, Supervision.

## Declaration of competing interest

The authors declare that they have no known competing financial interests or personal relationships that could have appeared to influence the work reported in this paper.

## Acknowledgment

This work was supported by the Scientific and Technological Research Council of Turkey (TUBITAK) under Grant no. 117E869.

## References

[1] Y. Saito, Y. Kishiyama, A. Benjebbour, T. Nakamura, A. Li, K. Higuchi, Non-orthogonal multiple access (NOMA) for cellular future radio access, in: 2013 IEEE 77th Vehicular Technology Conference, VTC Spring, 2013, pp. 1–5, http://dx.doi.org/10.1109/VTCSpring.2013.6692652.

[2] W. Shin, M. Vaezi, B. Lee, D.J. Love, J. Lee, H.V. Poor, Non-orthogonal multiple access in multi-cell networks: Theory, performance, and practical challenges, IEEE Commun. Mag. 55 (10) (2017) 176–183, http://dx.doi.org/10.1109/MCOM.2017.1601065.

[3] Z. Ding, Z. Yang, P. Fan, H.V. Poor, On the performance of non-orthogonal multiple access in 5G systems with randomly deployed users, IEEE Signal Process. Lett. 21 (12) (2014) 1501–1505, http://dx.doi.org/10.1109/LSP.2014.2343971.

[4] Z. Ding, M. Peng, H.V. Poor, Cooperative non-orthogonal multiple access in 5G systems, IEEE Commun. Lett. 19 (8) (2015) 1462–1465, http://dx.doi.org/10.1109/LCOMM.2015.2441064.

[5] J. Men, J. Ge, Non-orthogonal multiple access for multiple-antenna relaying networks, IEEE Commun. Lett. 19 (10) (2015) 1686–1689, http://dx.doi.org/10.1109/LCOMM.2015.2472006.

[6] X. Liang, Y. Wu, D.W.K. Ng, Y. Zuo, S. Jin, H. Zhu, Outage performance for cooperative NOMA transmission with an AF relay, IEEE Commun. Lett. 21 (11) (2017) 2428–2431, http://dx.doi.org/10.1109/LCOMM.2017.2681661.

[7] J. Men, J. Ge, C. Zhang, Performance analysis of nonorthogonal multiple access for relaying networks over Nakagami-*m* fading channels, IEEE Trans. Veh. Technol. 66 (2) (2017) 1200–1208, http://dx.doi.org/10.1109/TVT.2016.2555399.

[8] J. Kim, I. Lee, Non-orthogonal multiple access in coordinated direct and relay transmission, IEEE Commun. Lett. 19 (11) (2015) 2037–2040, http://dx.doi.org/10.1109/LCOMM.2015.2474856.

[9] Z. Ding, H. Dai, H.V. Poor, Relay selection for cooperative NOMA, IEEE Wirel. Commun. Lett. 5 (4) (2016) 416–419, http://dx.doi.org/10.1109/LWC.2016.2574709.

[10] Z. Yang, Z. Ding, Y. Wu, P. Fan, Novel relay selection strategies for cooperative NOMA, IEEE Trans. Veh. Technol. 66 (11) (2017) 10114–10123, http://dx.doi.org/10.1109/TVT.2017.2752264.

[11] X. Wang, F. Labeau, L. Mei, Closed-form BER expressions of QPSK constellation for uplink non-orthogonal multiple access, IEEE Commun. Lett. 21 (10) (2017) 2242–2245, http://dx.doi.org/10.1109/LCOMM.2017.2720583.

[12] F. Kara, H. Kaya, BER performances of downlink and uplink NOMA in the presence of SIC errors over fading channels, IET Commun. 12 (15) (2018) 1834–1844, http://dx.doi.org/10.1049/iet-com.2018.5278.

[13] L. Bariah, S. Muhaidat, A. Al-Dweik, Error probability analysis of non-orthogonal multiple access over Nakagami- *m* fading channels, IEEE Trans. Commun. 67 (2) (2019) 1586–1599, http://dx.doi.org/10.1109/TCOMM.2018.2876867.

[14] E. Basar, Index modulation techniques for 5G wireless networks, IEEE Commun. Mag. 54 (7) (2016) 168–175, http://dx.doi.org/10.1109/MCOM.2016.7509396.

[15] E. Basar, M. Wen, R. Mesleh, M. Di Renzo, Y. Xiao, H. Haas, Index modulation techniques for next-generation wireless networks, IEEE Access 5 (2017) 16693–16746, http://dx.doi.org/10.1109/ACCESS.2017.2737528.

[16] R.Y. Mesleh, H. Haas, S. Sinanovic, C.W. Ahn, S. Yun, Spatial modulation, IEEE Trans. Veh. Technol. 57 (4) (2008) 2228–2241, http://dx.doi.org/10.1109/TVT.2007.912136.

[17] J. Jeganathan, A. Ghrayeb, L. Szczecinski, A. Ceron, Space shift keying modulation for MIMO channels, IEEE Trans. Wireless Commun. 8 (7) (2009) 3692–3703, http://dx.doi.org/10.1109/TWC.2009.080910.

[18] X. Zhu, Z. Wang, J. Cao, NOMA-Based spatial modulation, IEEE Access 5 (2017) 3790–3800, http://dx.doi.org/10.1109/ACCESS.2017.2688019.

[19] J.W. Kim, S.Y. Shin, V.C.M. Leung, Performance enhancement of downlink NOMA by combination with GSSK, IEEE Wirel. Commun. Lett. 7 (5) (2018) 860–863, http://dx.doi.org/10.1109/LWC.2018.2833469.

[20] C. Zhong, X. Hu, X. Chen, D.W.K. Ng, Z. Zhang, Spatial modulation assisted multi-antenna non-orthogonal multiple access, IEEE Wirel. Commun. 25 (2) (2018) 61–67, http://dx.doi.org/10.1109/MWC.2018.1700062.

[21] R.F. Siregar, F.W. Murti, S.Y. Shin, Combination of spatial modulation and non-orthogonal multiple access using hybrid detection scheme, in: 2017 Ninth International Conference on Ubiquitous and Future Networks, ICUFN, 2017, pp. 476–481, http://dx.doi.org/10.1109/ICUFN.2017.7993830.

[22] Q. Li, M. Wen, E. Basar, H.V. Poor, F. Chen, Spatial modulation-aided cooperative NOMA: Performance analysis and comparative study, IEEE J. Sel. Top. Sign. Proces. 13 (3) (2019) 715–728, http://dx.doi.org/10.1109/JSTSP.2019.2898099.

[23] A.K. Khandani, Media-based modulation: Converting static Rayleigh fading to AWGN, in: 2014 IEEE International Symposium on Information Theory, 2014, pp. 1549–1553, http://dx.doi.org/10.1109/ISIT.2014.6875093.

[24] E. Basar, Media-based modulation for future wireless systems: A tutorial, IEEE Wirel. Commun. 26 (5) (2019) 160–166, http://dx.doi.org/10.1109/MWC.2019.1800568.

[25] Y. Naresh, A. Chockalingam, On media-based modulation using RF mirrors, IEEE Trans. Veh. Technol. 66 (6) (2017) 4967–4983, http://dx.doi.org/10.1109/TVT.2016.2620989.

[26] Z. Bouida, H. El-Sallabi, M. Abdallah, A. Ghrayeb, K.A. Qaraqe, Reconfigurable antenna-based space-shift keying for spectrum sharing systems under Rician fading, IEEE Trans. Commun. 64 (9) (2016) 3970–3980, http://dx.doi.org/10.1109/TCOMM.2016.2590543.

[27] E. Basar, I. Altunbas, Space-time channel modulation, IEEE Trans. Veh. Technol. 66 (8) (2017) 7609–7614, http://dx.doi.org/10.1109/TVT.2017.2674689.

[28] I. Yildirim, E. Basar, I. Altunbas, Quadrature channel modulation, IEEE Wirel. Commun. Lett. 6 (6) (2017) 790–793, http://dx.doi.org/10.1109/LWC.2017.2742508.
[29] B. Shamasundar, S. Jacob, L.N. Theagarajan, A. Chockalingam, Media-based modulation for the uplink in massive MIMO systems, IEEE Trans. Veh. Technol. 67 (9) (2018) 8169–8183, http://dx.doi.org/10.1109/TVT.2018.2839706.
[30] M. Hasan, I. Bahceci, M.A. Towfiq, T.M. Duman, B.A. Cetiner, Mode shift keying for reconfigurable MIMO antennas: Performance analysis and antenna design, IEEE Trans. Veh. Technol. 68 (1) (2019) 320–334, http://dx.doi.org/10.1109/TVT.2018.2878768.
[31] P. Som, A. Chockalingam, Decode-and-forward cooperative multicast with space shift keying, in: 2014 IEEE Wireless Communications and Networking Conference, WCNC, 2014, pp. 689–694, http://dx.doi.org/10.1109/WCNC.2014.6952131.
[32] P. Som, A. Chockalingam, Performance analysis of space-shift keying in decode-and-forward multihop MIMO networks, IEEE Trans. Veh. Technol. 64 (1) (2015) 132–146, http://dx.doi.org/10.1109/TVT.2014.2318437.
[33] R. Mesleh, S.S. Ikki, Performance analysis of spatial modulation with multiple decode and forward relays, IEEE Wirel. Commun. Lett. 2 (4) (2013) 423–426, http://dx.doi.org/10.1109/WCL.2013.051513.130256.
[34] G. Altın, E. Basar, U. Aygölü, M.E. Çelebi, Performance analysis of cooperative spatial modulation with multiple-antennas at relay, in: 2016 IEEE International Black Sea Conference on Communications and Networking, BlackSeaCom, 2016, pp. 1–5, http://dx.doi.org/10.1109/BlackSeaCom.2016.7901557.
[35] F. Yarkin, I. Altunbas, E. Basar, Cooperative space shift keying media-based modulation with hybrid relaying, IEEE Syst. J. (2019) 1–10, http://dx.doi.org/10.1109/JSYST.2019.2899876.
[36] Y. Naresh, A. Chockalingam, Full-duplex media-based modulation, in: 2017 IEEE Globecom Workshops, GC Wkshps, 2017, pp. 1–6, http://dx.doi.org/10.1109/GLOCOMW.2017.8269129.
[37] S. Timotheou, I. Krikidis, Fairness for non-orthogonal multiple access in 5G systems, IEEE Signal Process. Lett. 22 (10) (2015) 1647–1651, http://dx.doi.org/10.1109/LSP.2015.2417119.
[38] Z. Yang, Z. Ding, P. Fan, N. Al-Dhahir, A general power allocation scheme to guarantee quality of service in downlink and uplink NOMA systems, IEEE Trans. Wireless Commun. 15 (11) (2016) 7244–7257, http://dx.doi.org/10.1109/TWC.2016.2599521.
[39] J.G. Proakis, M. Salehi, Digital Communications, McGraw-Hill, 2008.
[40] M.K. Simon, M.S. Alouini, Digital Communication over Fading Channels, Wiley, 2005.
[41] I.S. Gradshteyn, I.M. Ryzhik, Table of Integrals, Series, and Products, seventh ed., Academic Press, New York, 2007.
[42] Z. Wang, G.B. Giannakis, A simple and general parameterization quantifying performance in fading channels, IEEE Trans. Commun. 51 (8) (2003) 1389–1398, http://dx.doi.org/10.1109/TCOMM.2003.815053.

**Mehmet Can** received the B.Sc. and M.Sc. degrees, all in electronics and communication engineering, from Istanbul Technical University, Istanbul, Turkey, in 2016 and 2019, respectively. Currently, he is a Ph.D. student and research assistant at Istanbul Technical University, Electronics and Communication Engineering Department. His research interests include MIMO systems, cooperative communication, index modulation and NOMA.

**İbrahim Altunbaş** was born in Sütçüler, Isparta, Turkey, in 1967. He received the B.Sc., M.Sc. and Ph.D. degrees, all in electronics and communication engineering, from the Istanbul Technical University, Istanbul, Turkey, in 1988, 1992 and 1999, respectively. From 1992 to 1999, he was a Research Assistant, from 1999 to 2006, he was an Assistant Professor and from 2006 to 2011 he was an Associate Professor at the Istanbul Technical University. He is currently a Professor at the same university. Between January 2001–November 2001, he was a Visiting Researcher at Texas A&M University, USA. Between November 2001–September 2002 and June 2015–August 2015, he was a Postdoctoral Fellow and a Visiting Researcher, respectively at the University of Ottawa, Canada. His research interests include digital communications, information theory, error control coding and modulation, turbo coding, LDPC coding, iterative decoding, polar coding, MIMO systems, space–time coding, cooperative communication, network coding, spatial modulation, index modulation, full-duplex communication, NOMA, energy harvesting, SWIPT, vehicular communication and channel modulation.

**Ertugrul Basar** received the B.S. degree (Hons.) from Istanbul University, Turkey, in 2007, and the M.S. and Ph.D. degrees from Istanbul Technical University, Turkey, in 2009 and 2013, respectively. He is currently an Associate Professor with the Department of Electrical and Electronics Engineering, Koç University, Istanbul, Turkey and the director of Communications Research and Innovation Laboratory (CoreLab). His primary research interests include MIMO systems, index modulation, waveform design, visible light communications, and signal processing for communications.

Recent recognition of his research includes the Science Academy (Turkey) Young Scientists (BAGEP) Award in 2018, Mustafa Parlar Foundation Research Encouragement Award in 2018, Turkish Academy of Sciences Outstanding Young Scientist (TUBA-GEBIP) Award in 2017, and the first-ever IEEE Turkey Research Encouragement Award in 2017.

Dr. Basar currently serves as an Editor of the IEEE TRANSACTIONS ON COMMUNICATIONS and Physical Communication (Elsevier), and as an Associate Editor of the IEEE COMMUNICATIONS LETTERS. He served as an Associate Editor for the IEEE ACCESS from 2016 to 2018.